THE JOURNAL OF PHYSICAL CHEMISTRY B

Article

pubs.acs.org/JPCB

Amyloid β-Protein Assembly: The Effect of Molecular Tweezers CLR01 and CLR03

Xueyun Zheng,[†] Deyu Liu,[†] Frank-Gerrit Klärner,[‡] Thomas Schrader,[‡] Gal Bitan,[§] and Michael T. Bowers*,[†]

[†]Department of Chemistry and Biochemistry, University of California, Santa Barbara, California 93106, United States

[‡]Institute of Organic Chemistry, University of Duisburg-Essen, Essen 45117, Germany

[§]Department of Neurology, David Geffen School of Medicine, Brain Research Institute, and Molecular Biology Institute, University of California at Los Angeles, Los Angeles, California 90095, United States

Supporting Information

ABSTRACT: The early oligomerization of amyloid β-protein (Aβ) has been shown to be an important event in the pathology of Alzheimer's disease (AD). Designing small molecule inhibitors targeting Aβ oligomerization is one attractive and promising strategy for AD treatment. Here we used ion mobility spectrometry coupled to mass spectrometry (IMS-MS) to study the different effects of the molecular tweezers CLR01 and CLR03 on Aβ self-assembly. CLR01 was found to bind to Aβ directly and disrupt its early oligomerization. Moreover, CLR01 remodeled the early oligomerization of Aβ42 by compacting the structures of dimers and tetramers and as a consequence eliminated higher-order oligomers. Unexpectedly, the negative-control derivative, CLR03, which lacks the hydrophobic arms of the tweezer structure, was found to facilitate early Aβ oligomerization. Our study provides an example of IMS as a powerful tool to study and better understand the interaction between small molecule modulators and Aβ oligomerization, which is not attainable by other methods, and provides important insights into therapeutic development of molecular tweezers for AD treatment.

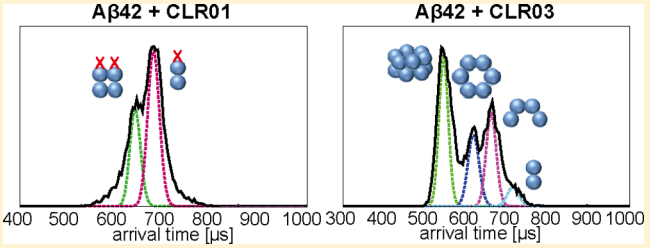

INTRODUCTION

Alzheimer's disease (AD) is the most common form of dementia, affecting over 44 million people worldwide.[1] AD is a progressive brain disorder that damages synapses and brain cells and causes decline of memory, loss of cognitive and executive functions, and eventually death.[2] There is no known cure for AD, and the etiology of the disease is not well understood. Previous studies have shown that amyloid β-protein (Aβ) plays an important role in AD pathogenesis.[3] Aβ is, in reality, not one but a group of peptides derived from the type-1 transmembrane protein, amyloid β-protein precursor (APP), through cleavage by β- and γ-secretases.

Aβ exists *in vivo* primarily as 40 or 42 amino acid long peptides with Aβ40 constituting 90% and Aβ42 ∼9% of all Aβ species.[4] Even though Aβ42 is a relatively minor constituent, it has been found to be the primary component of amyloid plaques, which are an important pathologic hallmark of AD.[5] In the plaques, Aβ is found as fibrillar, β-sheet-rich aggregates. Formation of Aβ fibrils *in vitro* and *in vivo* is a complex process involving multiple intermediate oligomeric species, which are highly neurotoxic and are believed to be the proximal neurotoxins acting in AD.[6−9] Immediately upon dissolution *in vitro*, Aβ42 forms small oligomers, including dimers and tetramers, as well as paranuclei (pentamers and hexamers) that self-associate to form decamers and dodecamers.[10−12] Among these species, the 56 kDa dodecamer has been identified as a plausible cause of memory deficits in the AD brain[13] and in transgenic mice.[14] Thus, targeting and remodeling Aβ42 oligomers is a primary therapeutic strategy for AD.[15]

One strategy for AD treatment and prevention is preventing Aβ formation, which could be achieved by inhibiting or modulating the β- and/or γ-secretase enzymes.[16] However, this approach has been problematic because both secretases cleave substrates other than APP, which are important in other functional biological processes.[17−19] Another potential strategy is enhancing clearance of Aβ oligomers and aggregates from the brain.[20] This can be accomplished either by facilitating degradation of Aβ by proteases[21] or other clearance mechanisms, or by directly remodeling the aggregation of Aβ into clearance-prone structures using suitable peptides or small molecules.

Many natural proteins, peptides, and small molecules have been discovered to interact with Aβ and modulate Aβ self-assembly.[22] Among them, small molecules are particularly attractive as a direct therapeutic strategy for the treatment of

Received: January 22, 2015
Revised: March 5, 2015
Published: March 9, 2015

DOI: 10.1021/acs.jpcb.5b00692
J. Phys. Chem. B 2015, 119, 4831−4841

AD.[23,24] For instance, biologically active molecules from green-tea ((−)epigallocatechin-3-gallate, EGCG) or the Indian spice turmeric (curcumin) have been found to prevent Aβ aggregation and inhibit Aβ-induced toxicity.[25,26] Inositol stereoisomers have been found to interact with Aβ and attenuate its neurotoxic effects.[27,28] Z-Phe-Ala-diazomethylketone (PADK), which acts as a lysosomal modulator up-regulating the expression of cathepsin B in lysosomes, has been shown to interact with Aβ42 directly and modulate Aβ42 oligomerization.[29] C-terminal fragments of Aβ42 and many polyphenol molecules have been shown to inhibit Aβ oligomerization, aggregation, and toxicity,[30−34] and molecules have been specially designed to inhibit not only aggregation of Aβ but also its metal binding and oxidation.[35]

Molecular tweezers (MTs), which possess a torus-shaped cavity with a surrounding belt of alternating aromatic and aliphatic rings, were designed to serve as host molecules binding specifically to lysine and to a lesser extent to arginine residues.[36−38] MTs were shown to be modulators of the aggregation of Aβ and other amyloidogenic proteins and effective inhibitors of the toxicity of these proteins.[39] A lead MT derivative, CLR01 (Figure 1a), was shown to inhibit the toxicity of multiple amyloidogenic proteins in cell viability assays using cell lines and primary cell cultures[39−42] and protected synaptic integrity and function of hippocampal and cortical neurons against the synaptotoxicity of Aβ42.[41] In addition, peripheral administration of CLR01 in transgenic mice led to a decrease in amyloid plaques, neurofibrillary tangles, and brain inflammation, suggesting that it is a promising candidate for therapeutic development.[41]

Mechanistic investigation showed that disruption of Aβ self-assembly is mediated by CLR01 binding to the two lysine and the single arginine residues in Aβ.[39] Dynamic light scattering (DLS) and electron microscopy (EM) experiments suggested that CLR01 does not prevent oligomer formation but rather modulates Aβ self-assembly into formation of structures that are neither amyloidogenic nor toxic.[39] Interestingly, by the relatively low resolution of DLS and EM, these structures were similar in size to the toxic and amyloidogenic oligomers of Aβ alone, suggesting that subtle conformational changes in Aβ might account for the apparent loss of amyloidogenic potential and toxic activity. However, the low-resolution methods could not provide information about what these changes might be. In addition, whether CLR01 binds Aβ monomers, oligomers, and/or larger aggregates has not been demonstrated directly.

In several previous studies, a derivative called CLR03 (Figure 1b) was used as a negative control.[39,41] This compound shares the polar bridgehead structure with CLR01 but lacks the hydrophobic arms, and therefore is not expected to bind specifically to lysine or arginine. Consequently, CLR03 indeed acted as a negative control and was not found to inhibit the aggregation and/or toxicity of amyloidogenic proteins. Nonetheless, how CLR03 interacts with Aβ and whether it has any effect on early Aβ oligomerization of Aβ remains to be uncovered.

To address all these questions, here we used ion mobility spectrometry coupled mass spectrometry (IMS-MS)[43,44] to investigate the effect of CLR01 and CLR03 on Aβ assembly. IMS-MS has been utilized successfully in the past to study Aβ and amyloid assembly[12,45−49] and the effects of various small molecules on the assembly process.[29,32,35,50]

EXPERIMENTAL METHODS

Peptide and Sample Preparation. Full-length Aβ40 and Aβ42 were synthesized by *N*-9-fluorenylmethoxycarbonyl (FMOC) chemistry. The peptides were purified by reverse-phase HPLC and their integrity validated by mass spectrometry and amino acid analysis as described previously.[51]

The samples were prepared in 10 mM ammonium acetate, and the pH was adjusted to 7.4. Samples contained 10 μM Aβ42 and molecular tweezers at different concentration ratios. An Aβ42 sample without MTs was prepared under the same procedure as a positive control.

Transmission Electron Microscopy (TEM). Microscopic analysis was performed using a FEI T-20 transmission electron microscope operating at 200 kV. The Aβ samples with and without molecular tweezers were prepared using the same procedure as that for the mass spectrometry analysis. The samples were kept at 4 °C for 2 weeks. For TEM measurements, 10 μL aliquots of samples were spotted on glow-discharged, carbon-coated copper grids (Ted Pella, Inc.). The samples were stained with 10 mM sodium metatungstate for 10 min and gently rinsed twice with deionized water. The sample grids were then dried at room temperature before TEM analysis.

Mass Spectrometry and Ion Mobility Spectrometry Analysis. Samples were analyzed on a home-built ion mobility spectrometry-mass spectrometer[43] which is composed of a nanoelectrospray ionization (nano-ESI) source, an ion funnel, a temperature-controlled drift cell, and a quadrupole mass filter followed by an electron multiplier for ion detection.

Briefly, for ion-mobility measurements, ions are generated continuously by a nano-ESI source, focused and stored in the ion funnel. A pulse of ions is injected into a temperature-controlled drift cell filled with 3−5 Torr helium gas, where they gently pass through under the influence of a weak electric field. The injection energy can be varied from ∼20 to ∼150 eV, but it is usually kept as low as possible to minimize thermal heating of the ions during the injection process. The ions exiting the drift cell are mass analyzed with a quadrupole mass filter, detected by the conversion dynode and channel electron multiplier, and recorded as a function of their arrival time distribution (ATD).

The ions in the drift cell experience a constant force from the electric field, E. This force is balanced by a retarding frictional force due to collisions with the buffer gas, resulting in a constant drift velocity, v_d. The drift velocity is proportional to the electric field:

$$v_d = KE \tag{1}$$

Here, the proportionality constant K is termed the ion mobility. The absolute ion mobility is dependent on the temperature (T) and the pressure (P) of the buffer gas, so it is typically converted to the reduced mobility K_0:

$$K_0 = K\frac{P}{760}\frac{273.16}{T} \tag{2}$$

The ions exiting the drift cell are mass analyzed and detected as a function of the arrival time, t_A. The reduced mobility K_0 can be determined from the instrument parameters by using eq 3 and plotting t_A versus P/V[52]

$$t_A = \frac{l^2}{K_0}\frac{273.16}{760T}\frac{P}{V} + t_0 \tag{3}$$

DOI: 10.1021/acs.jpcb.5b00692
J. Phys. Chem. B 2015, 119, 4831−4841

In eq 3, l is the length of the drift cell (4.503 cm), V is the voltage across the drift cell, and t_0 is the time the ions spend outside the drift cell before hitting the detector. All of these quantities are either known constants or are measured for each experiment.

The reduced ion mobility K_0 can be related to the collision cross section Ω using kinetic theory[53]

$$K_0 = \frac{3q}{16N}\left(\frac{2\pi}{\mu k_B T}\right)^{1/2}\frac{1}{\Omega} \quad (4)$$

Here, q is the ion charge, N is the buffer gas number density at STP, μ is the reduced mass of the ion−He collision, and k_B is the Boltzmann constant. The measured reduced mobility (K_0) and the collision cross section (Ω) provide information about the three-dimensional configurations of the ions. For peptide and protein ions, the secondary and tertiary structural information and the oligomeric states can be identified by comparison with modeling.

Experimental arrival time distributions can be fitted by calculating the flux of ions exiting the drift tube using ion transport theory.[53] The ion packet is taken as a periodic delta function, and the flux is given by eq 5:

$$\Phi(0, z, t) = \frac{sae^{-\alpha t}}{4(\pi D_L t)^{1/2}}\left(v_d + \frac{z}{t}\right)[1 - e^{-r_0^2/4D_T t}] \times e^{-r_0^2/4D_T t} \quad (5)$$

Here z is the ion charge, r_0 is the radius of the initial ion packet, a is the area of the exit aperture, D_L and D_T are the longitudinal and transverse diffusion coefficients, s is the initial ion density, and α is the loss of ions due to reactions in the drift cell. The fitted feature represents the theoretical ATD for one species with a given cross section. If a feature in the experimental ATD is broader than the fitted one, then the feature possibly represents a family of structures, rather than a single structure.

RESULTS

For the IMS-MS experiments performed here, Aβ and the molecular tweezers were prepared in ammonium acetate buffer, in contrast to previous experiments in which they were studied in sodium phosphate buffer. This change in condition was not expected to cause major changes in Aβ assembly or its inhibition. To verify this expectation experimentally, we assessed samples of Aβ42 in the absence or presence of CLR01 or CLR03 by TEM. Aβ42 was incubated with CLR01 at 1:1 or 1:10 concentration ratio, respectively, and with CLR03 at 1:10 concentration ratio.

As shown in Figure S1 (Supporting Information), Aβ42 shows long fibrils in the absence of tweezers or in the presence of CLR03, as observed previously in sodium phosphate buffer.[39] In the presence of an equimolar concentration of CLR01, the Aβ42 sample shows a few protofibril-like structures and amorphous structures. At 1:10 Aβ42:CLR01 concentration, only small amorphous structures are observed. These TEM results show that CLR01 inhibits the fibril formation by Aβ42, whereas CLR03 does not, which is consistent with previous studies in sodium phosphate buffer. These results indicate that the change of buffer has a minimal effect on Aβ fibrillogenesis and the way it is impacted by CLR01 or CLR03, supporting the comparison between the data shown below and previous biophysical investigations of these systems.

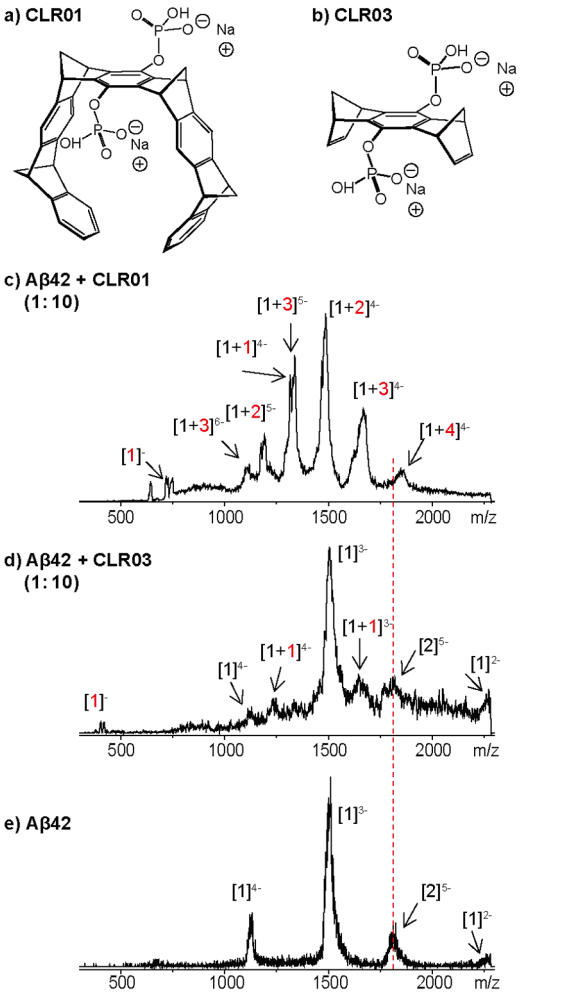

Figure 1. Different binding effects of CLR01 and CLR03 on Aβ42. (a, b) Molecular structures of CLR01 and CLR03 compounds; (c−e) mass spectra of Aβ42 samples: (c) 1:10 mixture of Aβ42 and CLR01; (d) 1:10 mixture of Aβ42 and CLR03; (e) Aβ42 alone. Each species is noted in brackets where the first number is the number of Aβ42 molecules and the second number represents the number of bound small molecules. The charge is noted as a superscript.

Mass Spectrometry Reveals Different Binding Effects of CLR01 and CLR03 on Aβ42. Mass spectra of Aβ42 samples in the absence or presence of MTs are shown in Figure 1. In the mass spectrum of Aβ42 alone (Figure 1e), there are four peaks, which correspond to Aβ42 species with charge states $z/n = -4, -3, -5/2$, and -2 (where z represents charge and n represents oligomer order), respectively, as described previously.[12,45] In the mass spectrum of a 1:10 mixture of Aβ42 and CLR01 (Figure 1c), there are three sets of peaks which correspond to -4, -5, and -6 charge states of the complexes of Aβ42 with one, two, three, or four CLR01 molecules bound. As the mass spectrometry study was conducted in negative ion mode, the binding form of CLR01 is with loss of sodium ions, which results in producing Aβ42 and CLR01 complexes with higher charge states. Note that no $-5/2$ Aβ42 peak (m/z = 1805), which represents dimer or higher order oligomers, is observed. This indicates that CLR01 disrupts the formation of Aβ42 dimers and higher order oligomers. No peaks of uncomplexed Aβ42 are observed in the mass spectrum, suggesting that CLR01 binds to Aβ42 directly with high

DOI: 10.1021/acs.jpcb.5b00692
J. Phys. Chem. B 2015, 119, 4831−4841

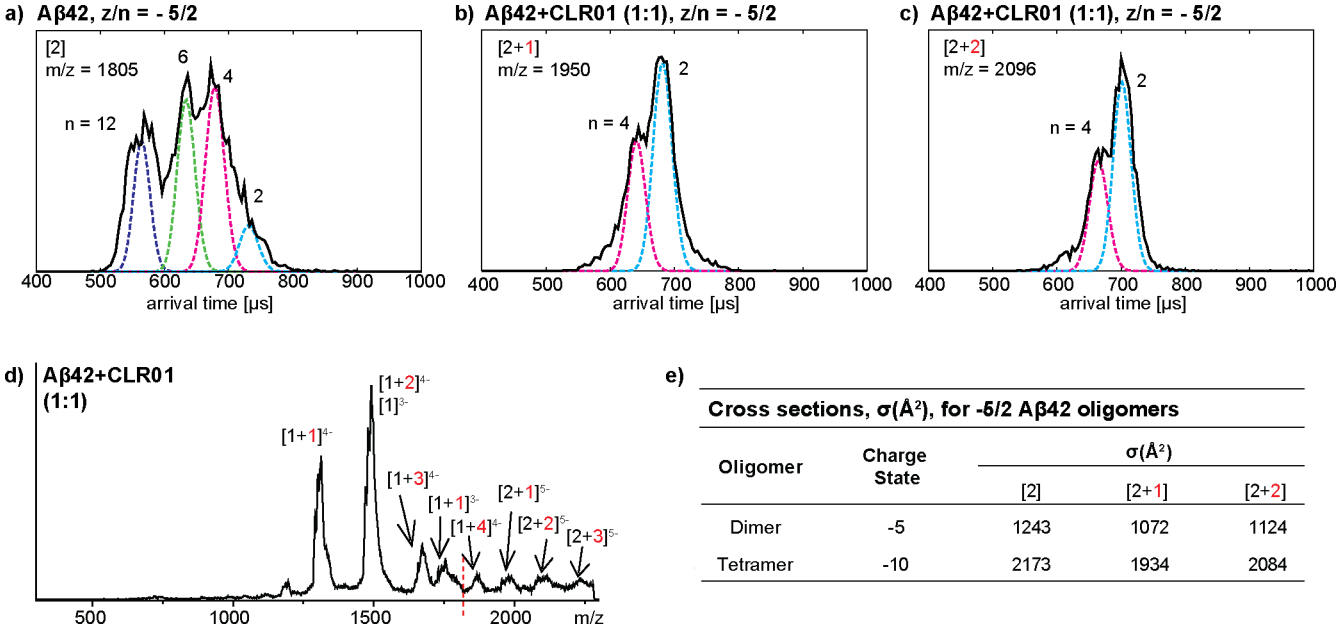

Cross sections, σ(Å²), for -5/2 Aβ42 oligomers

Oligomer	Charge State	σ(Å²)		
		[2]	[2+1]	[2+2]
Dimer	-5	1243	1072	1124
Tetramer	-10	2173	1934	2084

Figure 2. Effects of low concentration CLR01 on Aβ42 early oligomerization. ATDs of (a) $z/n = -5/2$ Aβ42 (m/z = 1805) in an Aβ42 sample without CLR01; (b) $z/n = -5/2$ Aβ42 and CLR01 complex (m/z = 1950); and (c) $z/n = -5/2$ Aβ42 and CLR01 complex (m/z = 2096) in a 1:1 mixture of Aβ42 and CLR01. Each ATD is fit with multiple features using the procedure described in the Experimental Methods section, and the oligomer order (n) is noted for each feature. (d) A mass spectrum of the 1:1 mixture of Aβ42 and CLR01 is shown as an example. Each species is noted in brackets where the first number is the number of Aβ42 molecules and the second number represents the number of bound CLR01 molecules. The charge is noted as a superscript. The dashed line represents the theoretical position for the uncomplexed −5/2 peak. Mass spectra of mixtures of Aβ42 and CLR01 with different ratios are shown in Figure S2 (Supporting Information). (e) Cross sections of dimer and tetramer in the uncomplexed or CLR01-complexed −5/2 Aβ42. The error for the cross sections reported here is between 0 and 1%.

affinity and there are no CLR01-free Aβ42 species present in solution.

In contrast, the spectrum of a 1:10 mixture of Aβ42 and CLR03 (Figure 1d) shows four peaks corresponding to the −4, −3, −5/2, and −2 Aβ42 species, similarly to Aβ42 alone (Figure 1e). There are two additional small peaks tailing the −3 and −4 Aβ42 peaks corresponding to the −3 and −4 complex species of Aβ42 with one CLR03 bound, respectively. The intensities of these two complex peaks are much lower than those with CLR01 bound, suggesting that the affinity of CLR03 binding to Aβ42 is much lower than that of CLR01.

To better understand the effects of CLR01 on Aβ42, the mass spectra of Aβ42 with different ratios of CLR01 (1:1, 1:2, 1:5, and 1:10) were recorded. The mass spectrum of a 1:1 mixture is shown in Figure 2d as an example, and others are provided in Figure S2 (Supporting Information). The mass spectrum of the 1:5 mixture of Aβ42 and CLR01 is similar to that of the 1:10 mixture (Figure 1c) with peaks corresponding to complex species Aβ42 and CLR01 with charge states −4, −5, and −6. As the concentration of CLR01 decreases (1:2 and 1:1 ratios), the complex species of Aβ42 and CLR01 with lower charge states (−4, −3, −5/2) are observed in the mass spectra. One possible explanation is that CLR01 itself is slightly basic in aqueous solution and the observed binding form of CLR01 is CLR01 with loss of sodium ions; therefore, the complexes tend to carry more charges in the presence of high concentration CLR01. Note that no z/n = −5/2 CLR01-free Aβ42 dimer peak is observed in any of the mixtures. However, in the low-ratio mixtures (1:1 and 1:2, see Figure 2d and Figure S2, Supporting Information), the −5/2 complex peaks of Aβ42 oligomers with CLR01 molecules bound are observed (m/z = 1950, 2096, and 2241 representing [2+**1**], [2+**2**], and [2+**3**] Aβ42−CLR01 complexes, respectively). These results suggest that CLR01 not only binds to Aβ42 monomers but also to small Aβ42 oligomers with relatively high affinity, thereby disrupting the formation of larger Aβ42 oligomers even at 1:1 ratio. As the concentration of CLR01 increases, the Aβ42 oligomers decrease in abundance or altogether disappear.

Ion Mobility Spectrometry Reveals CLR01 Inhibiting Early Aβ42 Oligomerization. To better understand the effects of CLR01 on Aβ42 oligomerization, an ion mobility study was conducted. No ATDs for the z/n = −5/2 Aβ42 peak (m/z = 1805) could be recorded, as it was not observed in any of the mixtures of Aβ42 and CLR01 (Figures 1c and 2d and Figure S2, Supporting Information). The ATDs of the [2+**1**] and [2+**2**] complex peaks were recorded and are shown in Figure 2b and c (the signal of [2 + 3] complex species was too weak to obtain a reliable ATD). The ATD of the −5/2 Aβ42 peak of pure Aβ42 (Figure 2a) shows four features with arrival times of ∼712, 680, 620, and 540 μs, which were previously assigned as Aβ42 dimer, tetramer, hexamer, and dodecamer, respectively, based on their cross section values (see refs 12 and 45 for a detailed discussion of the −5/2 peak assignment). In contrast, in the 1:1 mixture of Aβ42 and CLR01, the ATD of the m/z = 1950 peak (Figure 2b, labeled as [2+**1**] species) shows only two features with arrival times of 690 and 640 μs, which are assigned as dimer and tetramer, respectively. This indicates there is one CLR01 molecule bound to the Aβ42 dimer and two CLR01 molecules bound to the Aβ42 tetramer, respectively. No features at lower arrival times are observed, suggesting there are no Aβ42 hexamers, dodecamers, or other larger oligomers formed in the presence of CLR01. The ATD of the m/z = 2096 peak (Figure 2c, labeled as [2+**2**] species) also shows two dominant features with arrival times of ∼700 and 660 μs, which correspond to Aβ42 dimer and tetramer, respectively. This indicates that there are two CLR01 molecules

DOI: 10.1021/acs.jpcb.5b00692
J. Phys. Chem. B 2015, 119, 4831−4841

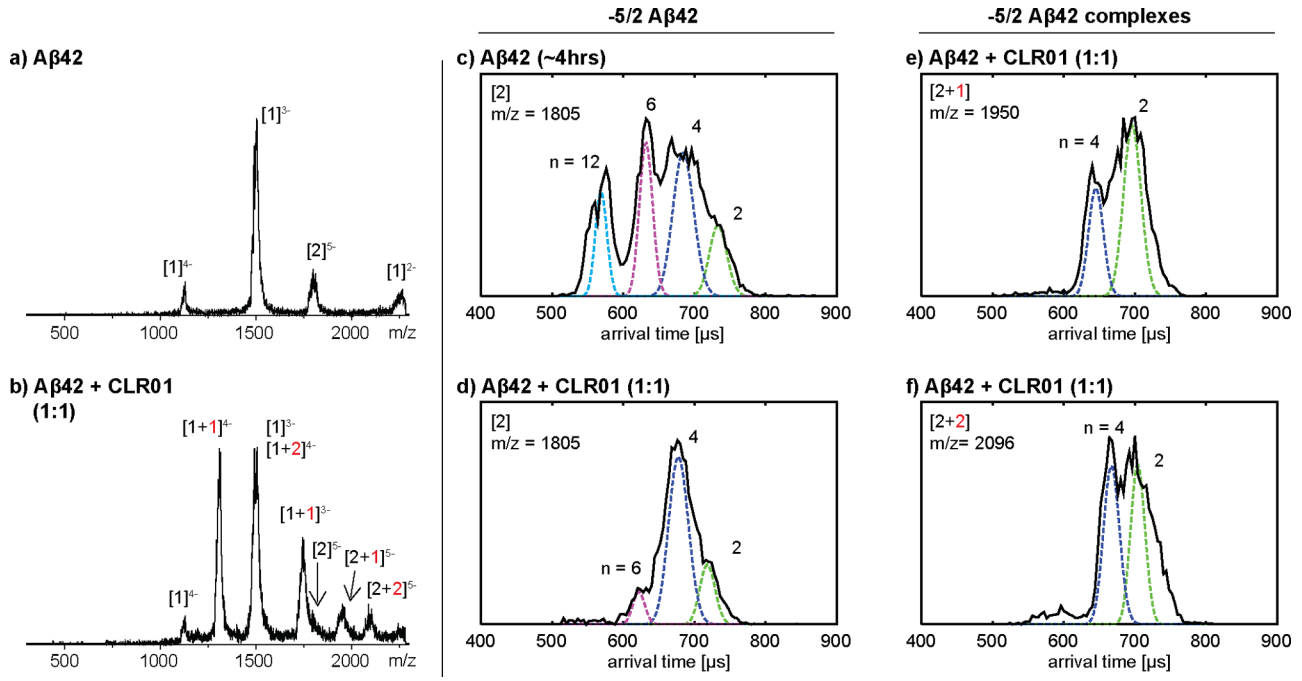

Figure 3. CLR01 remodels the early oligomerization of Aβ42. (a) Mass spectrum of Aβ42 alone with ~4 h of incubation on ice; (b) mass spectrum of the Aβ42 sample immediately after the addition of 1:1 CLR01. Each species is noted in brackets where the first number is the number of Aβ42 and the second number represents the number of bound CLR01 molecules. The charge is noted as a superscript. (c) ATD of the $z/n = -5/2$ Aβ42 peak for the Aβ42 in the absence of CLR01 after ~4 h of incubation on ice. (d) ATD of the $z/n = -5/2$ Aβ42 peak after addition of 1:1 CLR01. (e and f) ATDs of $-5/2$ Aβ42 oligomer complexes after addition of 1:1 CLR01 to the preaggregated Aβ42 sample. Each ATD is fit with multiple features using the procedure described in the Experimental Methods section, and the oligomer order (n) is noted for each feature.

bound to the Aβ42 dimer and four CLR01 molecules bound to the Aβ42 tetramer. Again, the highest oligomers with CLR01 bound observed are tetramers and absence of features at lower arrival times indicates no hexamer, dodecamer, or higher order oligomer formation. These results indicate that CLR01 not only binds to Aβ42 monomers but also to small oligomers and inhibits the formation of hexamer and higher order oligomers.

The cross sections of oligomer complexes are given in Figure 2e. Interestingly, the cross sections of dimers with one or two CLR01 molecules bound are significantly smaller than those of the dimer with no ligands attached, even though their mass has increased. This result suggests CLR01 induces more interaction between the two monomers, leading to a compact conformation and overall size reduction. Similarly, the cross sections of tetramers with two or four CLR01 molecules bound are smaller than those of the tetramer with no CLR01 bound. In addition, the tetramer ATD peaks with CLR01 bound (Figure 2b, c) are much narrower than in wild type Aβ42. This indicates there is little structure variation in the CLR01 bound tetramer while in wt Aβ42 the tetramer family of structures is both larger and more varied. The unbound Aβ42 tetramer normally adopts a family of structures that have a bent arrangement (~120° angle).[12] It is likely that the tetramers with CLR01 bound adopt either a more closed square ring structure or a pyramidal structure accounting for the fact they are smaller than CLR01-free Aβ42 tetramers and that dimer cannot be added to form hexamer. A similar effect prevents Aβ40 from growing beyond tetramer and explains its greatly reduced toxicity relative to Aβ42.[12]

CLR01 Remodels Preformed Aβ42 Oligomers. To explore whether CLR01 can remodel the early oligomerization of Aβ42 not only immediately upon dissolution but also after the oligomers have already formed, Aβ42 was incubated for 4 h on ice, following which CLR01 was added to the samples. The samples were incubated at a low temperature to allow quasi-equilibrium of small oligomers to be reached but avoid extensive aggregation, which happens at higher temperatures and leads to clogging of the nano-ESI capillaries, preventing further analysis. The results are shown in Figure 3.

Following incubation, the mass spectrum of Aβ42 (Figure 3a) shows four peaks with charge states of $z/n = -4, -3, -5/2$, and -2. The ATD of the $-5/2$ peak shows four features corresponding to dimer, tetramer, hexamer, and dodecamer, similar to Figure 2a. Upon addition of CLR01 at 1:1 concentration ratio, new peaks appeared corresponding to $z/n = -4, -3$ monomer complexes and $z/n = -5/2$ oligomer complexes (Figure 3b). Overall, the spectrum was similar to the one obtained in the inhibition study (Figure 2d), with the exception that no peaks were observed with 3 or 4 CLR01 molecules bound. The data indicate that CLR01 binds to Aβ42 monomers and preformed Aβ42 oligomers directly, mostly with 1:1 or 1:2 stroichiometry, whereas binding of additional CLR01 molecules is less likely after incubation. This suggests the existence of two main binding sites for CLR01 on Aβ, Lys16, and Lys28.[39]

Interestingly, the ATD of the $z/n = -5/2$ unbound Aβ42 peak (Figure 3d) showed only three features representing dimer, tetramer, and a small amount of hexamer after the addition of equimolar CLR01. The feature representing Aβ42 dodecamer was eliminated after the addition of CLR01, suggesting that the binding of CLR01 dissociated the preformed Aβ42 dodecamer. Moreover, the relative intensity of the hexamer decreased significantly compared to that before CLR01 addition (Figure 3c), suggesting CLR01 began to also dissociate hexamers. The ATDs of the $z/n = -5/2$ Aβ42:CLR01 oligomer complex peaks (Figure 3e, f) showed

DOI: 10.1021/acs.jpcb.5b00692
J. Phys. Chem. B 2015, 119, 4831−4841

only the two features corresponding to dimer and tetramer with CLR01 molecules bound, as observed immediately upon mixing of Aβ42 and CLR01 (Figure 2b and c), suggesting that binding of CLR01 to Aβ42 dimers or tetramers changes their structure so that additional dimers cannot be added to form hexamers. The ATDs of the z/n = −5/2 peaks were monitored again after 1 day of incubation at 4 °C, and the results (see Figure S3, Supporting Information) were similar to those obtained following 4 h of incubation, suggesting that CLR01 maintained the distribution of Aβ42 oligomers, in which dodecamers were excluded and hexamers were a minor species.

To test the effect of the Aβ42:CLR01 concentration ratio on the remodeling of Aβ42 oligomerization, higher ratios of CLR01 (1:5 and 1:10, respectively) were added to 4 h incubated Aβ42. The mass spectrum of the 1:5 mixture is shown in Figure S4c (Supporting Information) (the result of the 1:10 ratio was similar to that of the 1:5 mixture and therefore is not shown). The mass spectrum of the 1:5 mixture showed mostly complexes of Aβ42 monomer with CLR01 molecules. No z/n = −5/2 peak of CLR01-free or CLR01-complexed Aβ42 was observed. These results suggest that high concentrations of CLR01 dissociate preformed Aβ42 oligomers. Taken together, these results indicate that CLR01 remodels Aβ42 oligomerization both at low and high concentration ratios.

Ion Mobility Spectrometry of Aβ42 Monomer Complexes. The ATDs of z/n = −3 of Aβ42 monomer in the absence or presence of CLR01 (1:1) are shown in Figure S5 (Supporting Information). In the ATD of the −3 monomer peak of Aβ42 alone, there are two dominant peaks with arrival times of ∼640 and ∼680 μs, previously identified as a solvent-free conformer and a solution-like conformer, respectively.[49] The ATD for the −3 peak of Aβ42 complexed with one CLR01 molecule shows two similar features with arrival times of ∼668 and ∼712 μs. By analogy, these are assigned as the solvent-free and solution-like conformers of Aβ42 monomer with one CLR01 bound, respectively.

The ATDs of z/n = −4 and −5 complexes of Aβ42 with one, two, three, or four CLR01 molecules bound in a 1:5 mixture, respectively, are shown in Figure S6 (Supporting Information). Those for z/n = −4 have two features in their ATDs, and as the number of bound CLR01 molecules increases, the intensity of the compact, shorter-time feature increases, relative to the more extended, longer-time feature. Overall, there are no features with shorter arrival times detected which indicates that only monomer with CLR01 complexed is present in solution. The cross sections of the Aβ42:CLR01 monomer complexes are shown in Figure S6c (Supporting Information). Addition of each CLR01 ligand increases the size of the complex by an amount comparable to the size of CLR01, suggesting that no major structural transitions occur in the monomers upon CLR01 binding.

Effects of CLR01 on Aβ40 Assembly. Aβ40 has an identical sequence to that of Aβ42 except for absence of Ile41 and Ala42 residues at the C-terminus but has very different assembly and pathological properties. Thus, it is interesting to examine how CLR01 affects its early oligomerization in comparison to Aβ42. The mass spectra of Aβ40 alone and Aβ40 mixed with CLR01 at different ratios are provided in Figure S7 (Supporting Information). The mass spectrum of Aβ40 alone shows three peaks which correspond to z/n = −4, −3, and −5/2, similar to the spectrum of the Aβ42. The mass spectra of mixtures of Aβ40 and CLR01 at different ratios show sets of peaks at charge states −3, −4, −5, and −6 corresponding to Aβ40:CLR01 complexes. Up to four CLR01 molecules are observed bound to Aβ40. At lower CLR01 concentration (1:1 ratio, Figure S7b, Supporting Information), there are three z/n = −5/2 peaks at m/z = 1876, 2021, and 2167, corresponding to [2+**1**], [2+**2**], and [2+3] oligomer complexes of Aβ40 and CLR01. At higher concentrations of CLR01 (1:5 and 1:10 ratios), no −5/2 oligomer complexes were detected, suggesting that no dimer or higher-order oligomers formed.

The ATDs of these −5/2 oligomer peaks are shown in Figure 4 (the signal of the [2+3] complex was too weak to obtain a reliable ATD and therefore is not shown). The −5/2 peak of Aβ40 (m/z = 1731, Figure 4a) shows two features with arrival times of ∼690 and ∼620 μs which previously were assigned as Aβ40 dimer and tetramer (see ref 12 for a detailed discussion of the −5/2 peak assignment). For the 1:1 mixture of Aβ40 and CLR01, the ATDs of −5/2 [2+**1**] and [2+**2**] oligomer complexes (Figure 4b and c) show two primary features, which can be assigned as dimer and tetramer based on their cross sections. These results indicate that there are one or

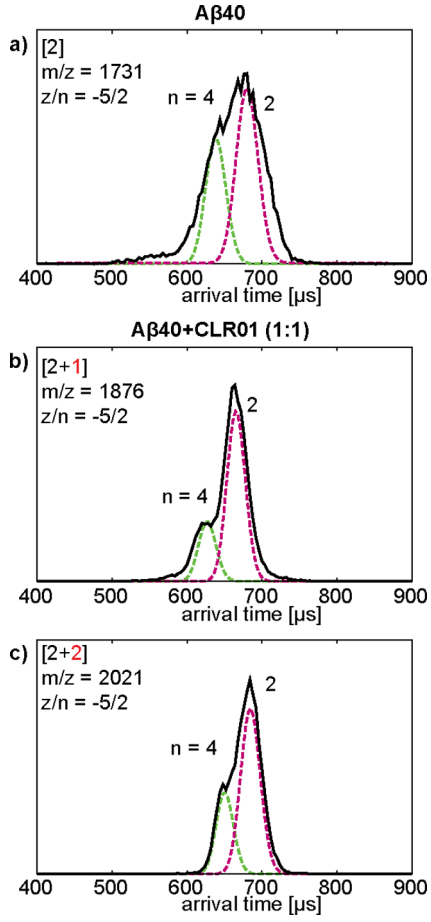

Figure 4. Effects of low concentration CLR01 on Aβ40 oligomerization. (a) ATD of z/n = −5/2 Aβ40 (m/z = 1731) for Aβ40 alone; (b and c) ATDs of z/n = −5/2 Aβ40 and CLR01 complexes (m/z = 1876 and 2021) in the 1:1 mixture of Aβ40 and CLR01. Each ATD is fit with multiple features using the procedure described in the Experimental Methods section, and the oligomer order (n) is noted for each feature. Note the ATDs with CLR01 bound, panels b and c, are significantly narrower than wild type, panel a.

DOI: 10.1021/acs.jpcb.5b00692
J. Phys. Chem. B 2015, 119, 4831−4841

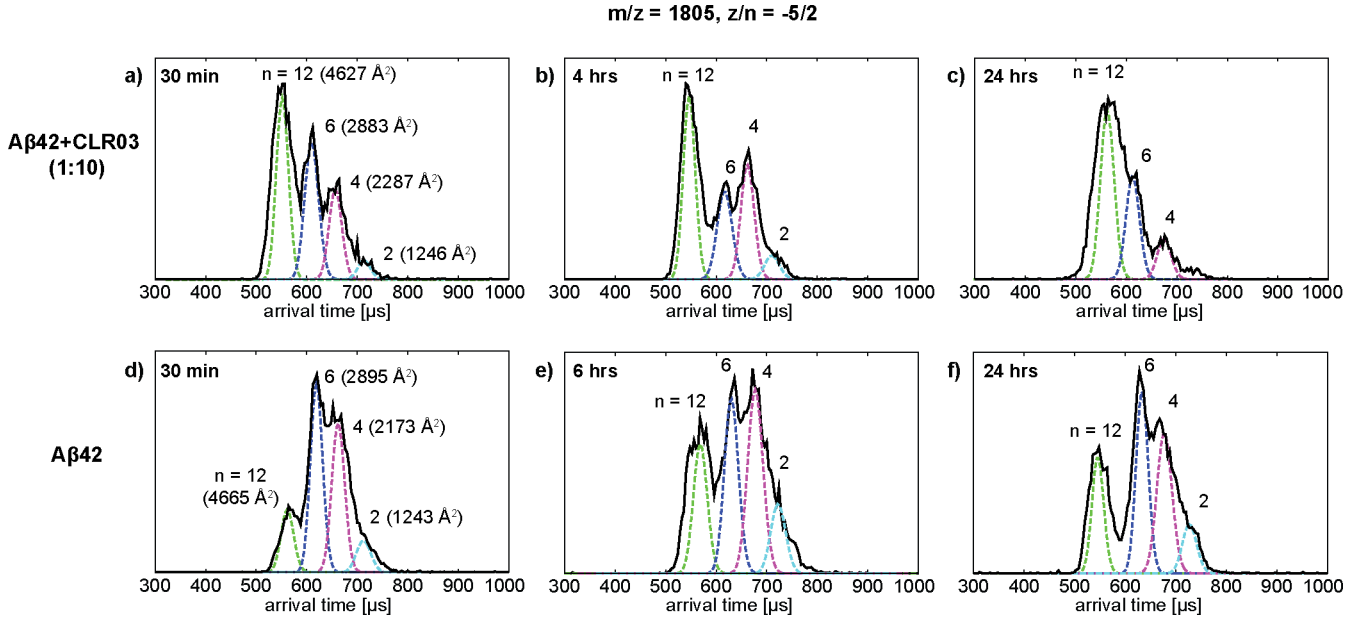

Figure 5. Time-dependent ion mobility study of the effects of CLR03 on Aβ42 early oligomerization. (a–c) ATDs of the −5/2 Aβ42 peak (m/z = 1805) for the 1:10 mixture of Aβ42 and CLR03 at different time points; (d–f) ATDs of the −5/2 Aβ42 peak (m/z = 1805) for Aβ42 alone at different time points. Each ATD is fit with multiple features using the procedure described in the Experimental Methods section. The oligomer order (n) and cross section are noted for each feature.

two CLR01 molecules bound to Aβ40 dimers and two or four CLR01 molecules bound to Aβ40 tetramers. No features at shorter arrival times were observed, indicating that there are no hexamer or larger oligomers formed. Interestingly, the intensities of the tetramer feature for [2+**1**] and [2+**2**] complex species (Figure 4b and c) are lower than that of the −5/2, CLR01-free Aβ40 tetramer feature, which indicates that the formation of tetramer is slower in the presence of CLR01 in the Aβ40 sample than in its absence.

The ATDs of monomer complexes with charge states z/n = −3, −4, −5, or −6 are shown in Figures S8 and S9 (Supporting Information). The z/n = −4 species (Figure S9a, Supporting Information) show two features in their ATDs corresponding to the solvent-free conformer and the solution-like conformer of Aβ40 complexed with CLR01. Taken together, these results indicate that CLR01 binds to Aβ40 with relatively high affinity and inhibits its early oligomerization. The cross sections of Aβ40 monomer complexes are shown in Figure S9b (Supporting Information). Similarly to the Aβ42 case, addition of each CLR01 ligand increases the size of the monomer complex by an amount comparable to the size of CLR01, suggesting that no major structural transitions occur in the monomers upon CLR01 binding.

IMS Reveals That CLR03 Facilitates Early Aβ42 Oligomerization. As noted above, CLR03 has been used as a negative-control compound, which was not expected to inhibit Aβ oligomerization or aggregation. Hence, we felt it was important to do similar experiments that are reported here.

A time-dependent study of the ATDs of the −5/2 Aβ42 peak (m/z = 1805) of Aβ42 alone and the 1:10 mixture of Aβ42 and CLR03 is shown in Figure 5. The ATD of the −5/2 Aβ42 peak for the 1:10 mixture of Aβ42 and CLR03 at 30 min (Figure 5a) shows four features that can be assigned as Aβ42 dimer, tetramer, hexamer, and dodecamer based on their cross sections, which is similar to the results of Aβ42 alone at 30 min (Figure 5d). Interestingly, the intensity of the dodecamer feature of the −5/2 peak for the mixture of Aβ42 and CLR03 is relatively higher than other features, whereas the intensity of the dodecamer feature of Aβ42 alone at 30 min is relatively lower than other features, suggesting that the growth of dodecamer in the presence of CLR03 is faster than in its absence. After up to 24 h of incubation, the dodecamer in the Aβ42 and CLR03 mixture becomes an even more dominant feature in the ATDs (Figure 5b and c), whereas the CLR01-free Aβ42 sample does not change substantially and appears to be in a state of quasi-equilibrium (Figure 5e and f). The observation of dodecamer and the significant rapid growth of dodecamer in the Aβ42 sample in the presence of CLR03 suggest that CLR03 not only does not inhibit the formation of Aβ42 dodecamer but actually facilitates the dodecamer formation.

ATDs of z/n = −3 and −4 peaks for Aβ42 alone and a 1:1 mixture of Aβ42 and CLR03 are shown in Figure 6. The ATD of the z/n = −3 Aβ42 peak for the mixture of Aβ42 and CLR03 (Figure 6b) shows two features at ∼640 and ∼680 μs corresponding to the compact and extended conformers, respectively, which is similar to those of Aβ42 alone (Figure 6a). Remarkably, there is another feature at a substantially shorter arrival time (∼500 μs) as noted by the arrow in addition to the two monomer features, which is not observed for Aβ42 alone. This indicates the presence of relatively large oligomers ($n \geq 2$) formed in the presence of CLR03. A similar feature is observed in the ATD of the z/n = −3 peak of Aβ42 with one CLR03 bound, which corresponds to large oligomers ($n \geq 2$). In Figure 6e and f, dominant features with shorter arrival times are observed in the ATDs for z/n = −4 peaks of Aβ42 with and without CLR03 bound, in addition to the monomer feature, indicating the presence of large oligomers ($n \geq 2$). These results are consistent with the results of the ATDs of the z/n = −5/2 Aβ42 peak (m/z = 1805, Figure 5) and further support the fact that CLR03 facilitates self-assembly of Aβ42.

DOI: 10.1021/acs.jpcb.5b00692
J. Phys. Chem. B 2015, 119, 4831−4841

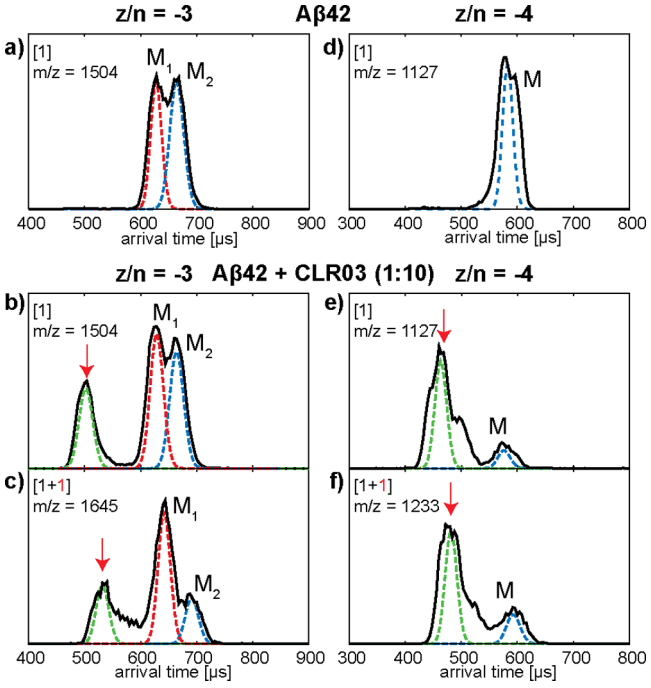

Figure 6. CLR03 facilitates Aβ42 oligomer formation: (a) ATD of the $z/n = -3$ peak for Aβ42 alone, (b and c) ATDs of $z/n = -3$ Aβ42 without and with CLR03 bound for a 1:10 mixture of Aβ42 and CLR03, (d) ATD of the $z/n = -4$ peak for Aβ42 alone, (e and f) $z/n = -4$ Aβ42 without and with CLR03 bound for a 1:10 mixture of Aβ42 and CLR03. Each ATD is fit with multiple features using the procedure described in the Experimental Methods section. M_1 and M_2 represent two conformations of the Aβ42 monomer. The arrows indicate the formation of oligomers ($n \geq 2$) in the mixture of Aβ42 and CLR03.

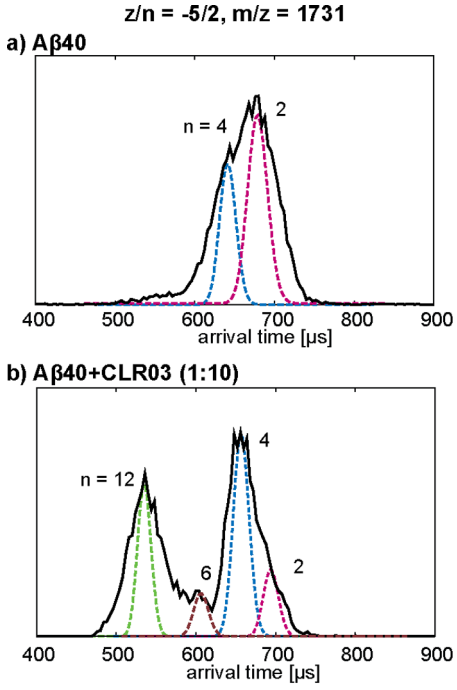

c) Cross sections for -5/2 Aβ40 oligomers

Charge State Oligomer	σ(Å²) -5 Dimer	σ(Å²) -10 Tetramer
Aβ40	1161	2084
Aβ40 + CLR01	1084*	1936*
Aβ40 + CLR03	1223	2215

* Cross sections of dimer with one CLR01 bound and tetramer with two CLR01 bound.

Figure 7. CLR03 facilitates Aβ40 assembly. (a, b) ATDs of the −5/2 Aβ40 peak (m/z = 1731) for the Aβ40 samples in the absence or presence of CLR03. Each ATD is fit with multiple features using the procedure described in the Experimental Methods section, and the oligomer order (n) is noted for each feature. (c) Cross sections of −5/2 Aβ40 oligomers for samples of Aβ40 in the absence or presence of CLR01 or CLR03. The error for the cross sections reported here is between 0 and 1%.

CLR03 Facilitates Aβ40 Assembly. The effect of CLR03 on Aβ40 oligomerization is shown in Figure 7. The mass spectrum of a 1:10 mixture of Aβ40 and CLR03 shows peaks corresponding to $z/n = -3$ and $z/n = -4$ monomer with one CLR03 bound but no CLR03 attachment to the $z/n = -5/2$ peak (Figure S10b, Supporting Information). However, the ATD of the −5/2 Aβ40 peak (m/z = 1731) in the presence of CLR03 (Figure 7b) shows formation of both Aβ40 hexamer and dodecamer based on their cross sections. In Figure 7c, the cross sections for the dimers and tetramers of Aβ40 are given for Aβ40 alone and for Aβ40 mixed with CLR01 and CLR03. Note that CLR03 significantly increases both cross sections, whereas CLR01 significantly decreases both cross sections. Further aggregation is enhanced by CLR03 and inhibited by CLR01.

The ATDs of $z/n = -3$ and -4 peaks of the 1:10 Aβ40:CLR03 mixture (Figure S11, Supporting Information) show features at arrival times shorter than those of monomers, suggesting formation of large oligomers ($n \geq 2$) in the presence of CLR03. Overall, these results reveal that CLR03 facilitates early oligomerization of Aβ40.

DISCUSSION AND CONCLUSIONS

Our mass spectrometry study of the lead molecular tweezer, CLR01, and the related derivative, CLR03, provides novel observations that could not have been obtained previously due to the low resolution of the methods used. Our investigation reveals that CLR01 and CLR03 bind to Aβ with very different affinities. Three CLR01 molecules bind with relatively higher affinity and a fourth weakly, but only one CLR03 molecule binds weakly to Aβ.

The Aβ:CLR01 stoichiometry found in our study is consistent with previous data suggesting that there are three possible binding sites for molecular tweezers on Aβ at Arg5, Lys16, and Lys 28.[39] Possible explanations for our observation of a fourth CLR01 molecule weakly binding to Aβ40 and Aβ42 could simply stem from differences in instrumentation, or might reflect nondiscriminating electrostatic and/or aromatic interactions between Aβ and CLR01 molecules, which might have been broken under harsher ionization conditions in the study by Sinha et al.[39] These nonspecific dispersive interactions could also explain the weak binding of one CLR03 molecule to Aβ, which was not observed within the limits of NMR detection in the previous study.[39]

The observation of three $z/n = -5/2$ oligomer complexes in the 1:1 and 1:2 mixtures of Aβ42 and CLR01, respectively, suggests that CLR01 not only binds to Aβ42 monomers but also to small Aβ42 oligomers (dimers and tetramers). Moreover, IMS reveals that CLR01 inhibits the formation of

DOI: 10.1021/acs.jpcb.5b00692
J. Phys. Chem. B 2015, 119, 4831−4841

hexamers and dodecamers. This is important, as dodecamers have been identified as probable toxic agents in AD.[12−14] Understanding the mechanism of how CLR01 blocks dodecamer formation is crucial for developing a therapeutic strategy for AD. Remarkably, the cross sections of the dimer and tetramer decreased substantially upon binding of CLR01 (see Figure 2e). These results suggest that CLR01 interacts with Aβ42 to change the folding of the monomer, which in turn changes the binding interface in dimer and tetramer formation, resulting in compact structures that resist further aggregation. Once multiple CLR01 ligands bind to the monomer, even dimer formation is prevented.

The ability of CLR01 to remodel early Aβ42 oligomerization after the oligomers had an opportunity to form and reach a quasi-equilibrium state for 4 h was assessed by IMS as well. Interestingly, even at low concentration (1:1 ratio), CLR01 was capable of removing preformed Aβ42 dodecamers and hexamers. At high concentrations (1:5 and 1:10 ratios), CLR01 removes essentially all preformed Aβ42 oligomers. These data are consistent with the inhibition results immediately upon mixing Aβ42 and CLR01. It is possible that CLR01 binds to Aβ42 monomers and oligomers and redirects them into either a slower aggregation process or an off-pathway set of structures. In either case, the resulting structures are nonamyloidogenic and nontoxic.[39−41] Our data reveal for the first time that the loss of amyloid-formation propensity and toxicity correlate with disruption of the oligomerization process and compaction of oligomers formed in the presence of CLR01.

Surprisingly, the related derivative, CLR03, was found to facilitate the early aggregation of Aβ42, especially promoting the formation of hexamers and dodecamers. Perhaps even more surprisingly, CLR03 also facilitated the formation of hexamers and dodecamers in Aβ40, which does not form these oligomers on its own. Previous studies showed that CLR03 did not inhibit Aβ42- or Aβ40-induced neurotoxicity.[39] However, how CLR03 interacts with Aβ has been unclear. Given the fact that CLR03 is an organic phosphate, we wondered whether it is possible the addition of CLR03 has a simple "salting out"-like effect, which would thereby promote Aβ aggregation. To address this possibility, an organic phosphate, *p*-nitrophenylphosphate (PNPP), was added to Aβ samples and was found not to induce significant changes in Aβ oligomerization (see Figure S12, Supporting Information). This result implies a simple "salting out"-like effect is not occurring for CLR03 and that CLR03 interacts with Aβ in a specific manner.

A major difference between the structures of CLR01 and CLR03 is that CLR01 has a torus-shaped cavity whereas CLR03 does not have a cavity structure. CLR03 carries a bridge-like structure with negatively charged phosphate groups on each side. It is possible that one of the phosphate groups on CLR03 interacts with positively charged residues (Lys, Arg, N-terminus) of Aβ through Coulombic interactions. The other phosphate group on the other side of CLR03 could then attract a positively charged residue of another Aβ or Aβ oligomer. Thus, by attracting positively charged residues in Aβ, CLR03 could facilitate Aβ oligomerization and aggregation.

Alternatively, CLR03 may interact weakly with two positively charged groups in a single Aβ, resulting in no observation of peaks for single Aβ with multiple CLR03 in the mass spectra (Figure 1d). As a consequence, conformation change may occur that promotes Aβ assembly. This is a form of salting out, and it may be more effective than PNPP. However, the fact that assembly is promoted to structures similar to wt Aβ42 speaks against salting out as a dominant assembly mechanism.

CLR01, which also carries two phosphate groups, however, does not catalyze Aβ oligomerization. This suggests that inclusion of lysine or arginine inside the cavity of CLR01 is of paramount importance for CLR01's mode of action. The central hydrophobic region of Aβ is regarded to be important for the hydrophobic clustering of Aβ. Recently, a macrocyclic inhibitor cucurbit[7]uril has been shown to inhibit amyloid fibrillation by hydrophobic interactions with nonpolar phenylalanine residues of Aβ.[54] CLR01, which has hydrophobic arms, is likely to have additional hydrophobic interactions with lysine residues. The binding of CLR01 to lysine residues, especially Lys16 which is close to the central hydrophobic region of Aβ, may result in conformation change of Aβ and compaction of Aβ oligomers. Our data suggest that binding of CLR01 causes Aβ monomers to either resist oligomer formation altogether or to redirect them to nontoxic oligomer assembly.

Previous detailed analysis showed that Aβ40 formed a nearly closed planar tetramer that resisted further dimer addition.[12] Here, we found that adding CLR01 to Aβ40 significantly reduced the cross sections of both the dimer and tetramer, leading to nearly isotropic assembly and reducing the likelihood of even forming the tetramer, much less higher-order oligomers. On the other hand, the presence of CLR03 in the solution significantly extended both the dimer and tetramer, yielding cross sections similar to those of the corresponding Aβ42 oligomers and leading to hexamer and dodecamer formation.

The essential features of these results are given in cartoon style in Figure 8. Aβ42 wt rapidly forms dodecamer, but addition of the molecular tweezer CLR01 eliminates dodecamer formation by inducing the dimer and tetramer to form compact species that cannot add additional Aβ42. The opposite

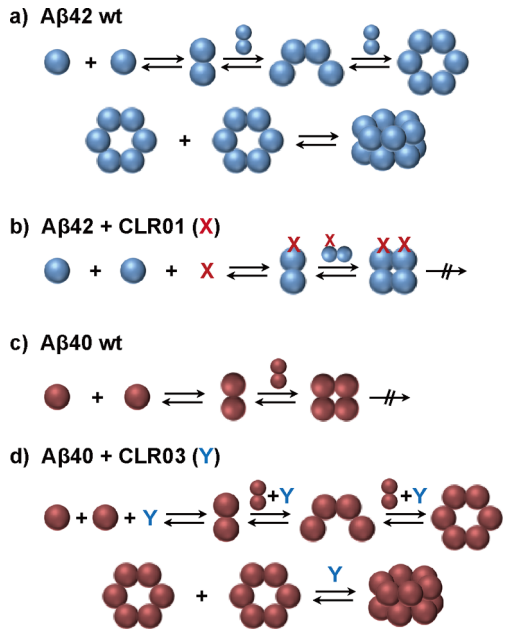

Figure 8. Different effects of CLR01 and CLR03 on Aβ early oligomerization. Oligomerization of (a) Aβ42 wild type, (b) Aβ42 with the presence of CLR01, (c) Aβ40 wild type, and (d) Aβ40 with the presence of CLR03. Aβ42 and Aβ40 are represented with blue and red balls, respectively. CLR01 and CLR03 molecules are noted as X and Y.

DOI: 10.1021/acs.jpcb.5b00692
J. Phys. Chem. B 2015, 119, 4831−4841

effect is obtained by CLR03. Aβ40 wt forms terminal compact tetramers, but addition of CLR03 leads to open tetramer formation and eventual dodecamer formation. These contrary effects are potentially of great importance in Aβ assembly and require further study to reveal the details involved. These studies, which will include both high level molecular dynamics modeling and additional direct sampling of structures of Aβ oligomers, are underway.

■ ASSOCIATED CONTENT

Supporting Information

TEM images, mass spectra of Aβ−MT mixtures, ATDs and cross sections of Aβ−MT complexes, and effects of PNPP on Aβ. This material is available free of charge via the Internet at http://pubs.acs.org.

■ AUTHOR INFORMATION

Corresponding Author

*E-mail: bowers@chem.ucsb.edu. Phone: 805-893-2893. Fax: 805-893-8703.

Notes

The authors declare the following competing financial interest(s): F.-G.K., T.S., and G.B. are co-authors and co-inventors of International Patent No. PCT/US2010/026419, USA Patent No. 8,791,092, and European Patent Application 10 708 075.6. G.B. is a Director and a Co-Founder of Clear Therapeutics, Inc..

■ ACKNOWLEDGMENTS

The work has been supported by the National Institutes of Health grant R01AG047116 (to M.T.B.), The UCLA Jim Easton Consortium for Drug Discovery and Biomarker Development (to G.B.), and National Science Foundation grant DMR-0805148 (to Galen D. Stucky). The Material Research Laboratory Shared Experimental Facilities are supported by the MRSEC Program of the NSF under Award No. DMR 1121053 (a member of the NSF-funded Materials Research Facilities Network, www.mrfn.org). We thank Margaret Condron at UCLA for synthesizing and purifying the Aβ40 and Aβ42 peptides used in this work.

■ REFERENCES

(1) Prince, M.; Albanese, E.; Guerchet, M.; Prina, M. *Alzheimer's Disease International: World Alzheimer Report*; 2014.

(2) Mattson, M. P. Pathways Towards and Away From Alzheimer's Disease. *Nature* **2004**, *430*, 631−639.

(3) Selkoe, D. J. Alzheimer's Disease: Genes, Proteins, and Therapy. *Physiol. Rev.* **2001**, *81*, 741−766.

(4) Jakob-Roetne, R.; Jacobsen, H. Alzheimer's Disease: From Pathology to Therapeutic Approaches. *Angew. Chem., Int. Ed.* **2009**, *48*, 3030−3059.

(5) Billings, L. M.; Oddo, S.; Green, K. N.; McGaugh, J. L.; LaFerla, F. M. Intraneuronal Aβ Causes the Onset of Early Alzheimer's Disease-related Cognitive Deficits in Transgenic Mice. *Neuron* **2005**, *45*, 675−688.

(6) Klein, W. L.; Krafft, G. A.; Finch, C. E. Targeting Small Aβ Oligomers: the Solution to an Alzheimer's Disease Conundrum? *Trends Neurosci.* **2001**, *24*, 219−224.

(7) Walsh, D. M.; Selkoe, D. J. Aβ Oligomers - a Decade of Discovery. *J. Neurochem.* **2007**, *101*, 1172−1184.

(8) Shankar, G. M.; Li, S. M.; Mehta, T. H.; Garcia-Munoz, A.; Shepardson, N. E.; Smith, I.; Brett, F. M.; Farrell, M. A.; Rowan, M. J.; Lemere, C. A.; et al. Amyloid-β Protein Dimers Isolated Directly From Alzheimer's Brains Impair Synaptic Plasticity and Memory. *Nat. Med.* **2008**, *14*, 837−842.

(9) Rahimi, F.; Shanmugam, A.; Bitan, G. Structure−Function Relationships of Pre-Fibrillar Protein Assemblies in Alzheimer's Disease and Related Disorders. *Curr. Alzheimer Res.* **2008**, *5*, 319−341.

(10) Bitan, G.; Kirkitadze, M. D.; Lomakin, A.; Vollers, S. S.; Benedek, G. B.; Teplow, D. B. Amyloid β-protein (Aβ) Assembly: Aβ40 and Aβ42 Oligomerize Through Distinct Pathways. *Proc. Natl. Acad. Sci. U. S. A.* **2003**, *100*, 330−335.

(11) Teplow, D. B.; Lazo, N. D.; Bitan, G.; Bernstein, S.; Wyttenbach, T.; Bowers, M. T.; Baumketner, A.; Shea, J. E.; Urbanc, B.; Cruz, L.; et al. Elucidating Amyloid β-Protein Folding and Assembly: A Multidisciplinary Approach. *Acc. Chem. Res.* **2006**, *39*, 635−645.

(12) Bernstein, S. L.; Dupuis, N. F.; Lazo, N. D.; Wyttenbach, T.; Condron, M. M.; Bitan, G.; Teplow, D. B.; Shea, J.-E.; Ruotolo, B. T.; Robinson, C. V.; et al. Amyloid-β Protein Oligomerization and the Importance of Tetramers and Dodecamers in the Aetiology of Alzheimer's Disease. *Nat. Chem.* **2009**, *1*, 326−331.

(13) Gong, Y.; Chang, L.; Viola, K. L.; Lacor, P. N.; Lambert, M. P.; Finch, C. E.; Krafft, G. A.; Klein, W. L. Alzheimer's Disease-Affected Brain: Presence of Oligomeric Aβ Ligands (ADDLs) Suggests a Molecular Basis for Reversible Memory Loss. *Proc. Natl. Acad. Sci. U. S. A.* **2003**, *100*, 10417−10422.

(14) Lesné, S.; Koh, M. T.; Kotilinek, L.; Kayed, R.; Glabe, C. G.; Yang, A.; Gallagher, M.; Ashe, K. H. A specific amyloid-β protein assembly in the brain impairs memory. *Nature* **2006**, *440*, 352−357.

(15) Liu, T.; Bitan, G. Modulating Self-assembly of Amyloidogenic Proteins as a Therapeutic Approach for Neurodegenerative Diseases: Strategies and Mechanisms. *ChemMedChem* **2012**, *7*, 359−374.

(16) Bateman, R. J.; Siemers, E. R.; Mawuenyega, K. G.; Wen, G.; Browning, K. R.; Sigurdson, W. C.; Yarasheski, K. E.; Friedrich, S. W.; DeMattos, R. B.; May, P. C.; et al. A γ-secretase Inhibitor Decreases Amyloid-β Production in The Central Nervous System. *Ann. Neurol.* **2009**, *66*, 48−54.

(17) Barten, D.; Meredith, J., Jr.; Zaczek, R.; Houston, J.; Albright, C. γ-Secretase Inhibitors for Alzheimer's Disease. *Drugs R&D* **2006**, *7*, 87−97.

(18) Imbimbo, P. B.; Giardina, G. A. M. γ-Secretase Inhibitors and Modulators for the Treatment of Alzheimer's Disease: Disappointments and Hopes. *Curr. Trends Med. Chem.* **2011**, *11*, 1555−1570.

(19) Ghosh, A. K.; Osswald, H. L. BACE1 (β-secretase) Inhibitors for the Treatment of Alzheimer's Disease. *Chem. Soc. Rev.* **2014**, *43*, 6765−6813.

(20) Bates, K. A.; Verdile, G.; Li, Q. X.; Ames, D.; Hudson, P.; Masters, C. L.; Martins, R. N. Clearance Mechanisms of Alzheimer's Amyloid-β Peptide: Implications for Therapeutic Design and Diagnostic Tests. *Mol. Psychiatry* **2009**, *14*, 469−486.

(21) Higuchi, M.; Iwata, N.; Saido, T. C. Understanding Molecular Mechanisms of Proteolysis in Alzheimer's Disease: Progress Toward Therapeutic Interventions. *Biochim. Biophys. Acta, Proteins Proteomic* **2005**, *1751*, 60−67.

(22) Stains, C. I.; Mondal, K.; Ghosh, I. Molecules that Target beta-Amyloid. *ChemMedChem* **2007**, *2*, 1675−1692.

(23) Necula, M.; Kayed, R.; Milton, S.; Glabe, C. G. Small Molecule Inhibitors of Aggregation Indicate That Amyloid β Oligomerization and Fibrillization Pathways Are Independent and Distinct. *J. Biol. Chem.* **2007**, *282*, 10311−10324.

(24) Hawkes, C. A.; Ng, V.; McLaurin, J. Small Molecule Inhibitors of Aβ-Aggregation and Neurotoxicity. *Drug Dev. Res.* **2009**, *70*, 111−124.

(25) Ehrnhoefer, D. E.; Bieschke, J.; Boeddrich, A.; Herbst, M.; Masino, L.; Lurz, R.; Engemann, S.; Pastore, A.; Wanker, E. E. EGCG Redirects Amyloidogenic Polypeptides into Unstructured, Off-pathway Oligomers. *Nat. Struct. Mol. Biol.* **2008**, *15*, 558−566.

(26) Yang, F. S.; Lim, G. P.; Begum, A. N.; Ubeda, O. J.; Simmons, M. R.; Ambegaokar, S. S.; Chen, P. P.; Kayed, R.; Glabe, C. G.; Frautschy, S. A.; et al. Curcumin Inhibits Formation of Amyloid β

DOI: 10.1021/acs.jpcb.5b00692
J. Phys. Chem. B 2015, 119, 4831−4841

Oligomers and Fibrils, Binds Plaques, and Reduces Amyloid In Vivo. *J. Biol. Chem.* **2005**, *280*, 5892−5901.
(27) McLaurin, J.; Golomb, R.; Jurewicz, A.; Antel, J. P.; Fraser, P. E. Inositol Stereoisomers Stabilize an Oligomeric Aggregate of Alzheimer Amyloid β Peptide and Inhibit Aβ-induced Toxicity. *J. Biol. Chem.* **2000**, *275*, 18495−18502.
(28) McLaurin, J.; Kierstead, M. E.; Brown, M. E.; Hawkes, C. A.; Lambermon, M. H.; Phinney, A. L.; Darabie, A. A.; Cousins, J. E.; French, J. E.; Lan, M. F.; et al. Cyclohexanehexol Inhibitors of Aβ Aggregation Prevent and Reverse Alzheimer Phenotype in a Mouse Model. *Nat. Med.* **2006**, *12*, 801−808.
(29) Zheng, X.; Gessel, M. M.; Wisniewski, M. L.; Viswanathan, K.; Wright, D. L.; Bahr, B. A.; Bowers, M. T. Z-Phe-Ala-diazomethylketone (PADK) Disrupts and Remodels Early Oligomer States of the Alzheimer Disease Aβ42 Protein. *J. Biol. Chem.* **2012**, *287*, 6084−6088.
(30) Fradinger, E. A.; Monien, B. H.; Urbanc, B.; Lomakin, A.; Tan, M.; Li, H.; Spring, S. M.; Condron, M. M.; Cruz, L.; Xie, C.-W.; et al. C-terminal Peptides Coassemble into Aβ42 Oligomers and Protect Neurons Against Aβ42-induced Neurotoxicity. *Proc. Natl. Acad. Sci. U. S. A.* **2008**, *105*, 14175−14180.
(31) Li, H.; Monien, B. H.; Lomakin, A.; Zemel, R.; Fradinger, E. A.; Tan, M.; Spring, S. M.; Urbanc, B.; Xie, C. W.; Benedek, G. B.; et al. Mechanistic Investigation of the Inhibition of Aβ42 Assembly and Neurotoxicity by Aβ42 C-Terminal Fragments. *Biochemistry* **2010**, *49*, 6358−6364.
(32) Gessel, M. M.; Wu, C.; Li, H.; Bitan, G.; Shea, J.-E.; Bowers, M. T. Aβ(39−42) Modulates Aβ Oligomerization but Not Fibril Formation. *Biochemistry* **2011**, *51*, 108−117.
(33) Porat, Y.; Abramowitz, A.; Gazit, E. Inhibition of Amyloid Fibril Formation by Polyphenols: Structural Similarity and Aromatic Interactions as a Common Inhibition Mechanism. *Chem. Biol. Drug Des.* **2006**, *67*, 27−37.
(34) Attar, A.; Rahimi, F.; Bitan, G. Modulators of Amyloid Protein Aggregation and Toxicity: EGCG and CLR01. *Transl. Neurosci.* **2013**, *4*, 385−409.
(35) Lee, S.; Zheng, X.; Krishnamoorthy, J.; Savelieff, M. G.; Park, H. M.; Brender, J. R.; Kim, J. H.; Derrick, J. S.; Kochi, A.; Lee, H. J.; et al. Rational Design of a Structural Framework with Potential Use to Develop Chemical Reagents That Target and Modulate Multiple Facets of Alzheimer's Disease. *J. Am. Chem. Soc.* **2014**, *136*, 299−310.
(36) Fokkens, M.; Schrader, T.; Klärner, F.-G. A Molecular Tweezer for Lysine and Arginine. *J. Am. Chem. Soc.* **2005**, *127*, 14415−14421.
(37) Klärner, F.-G.; Schrader, T. Aromatic Interactions by Molecular Tweezers and Clips in Chemical and Biological Systems. *Acc. Chem. Res.* **2012**, *46*, 967−978.
(38) Dutt, S.; Wilch, C.; Gersthagen, T.; Talbiersky, P.; Bravo-Rodriguez, K.; Hanni, M.; Sánchez-García, E.; Ochsenfeld, C.; Klärner, F.-G.; Schrader, T. Molecular Tweezers with Varying Anions: A Comparative Study. *J. Org. Chem.* **2013**, *78*, 6721−6734.
(39) Sinha, S.; Lopes, D. H.; Du, Z.; Pang, E. S.; Shanmugam, A.; Lomakin, A.; Talbiersky, P.; Tennstaedt, A.; McDaniel, K.; Bakshi, R.; et al. Lysine-Specific Molecular Tweezers are Broad-Spectrum Inhibitors of Assembly and Toxicity of Amyloid Proteins. *J. Am. Chem. Soc.* **2011**, *133*, 16958−16969.
(40) Sinha, S.; Du, Z.; Maiti, P.; Klärner, F. G.; Schrader, T.; Wang, C.; Bitan, G. Comparison of Three Amyloid Assembly Inhibitors: the Sugar Scyllo-Inositol, the Polyphenol Epigallocatechin Gallate, and the Molecular Tweezer CLR01. *ACS Chem. Neurosci.* **2012**, *3*, 451−458.
(41) Prabhudesai, S.; Sinha, S.; Attar, A.; Kotagiri, A.; Fitzmaurice, A. G.; Lakshmanan, R.; Ivanova, M. I.; Loo, J. A.; Klärner, F. G.; Schrader, T.; et al. A Novel "Molecular Tweezer" Inhibitor of α-Synuclein Neurotoxicity In Vitro and In Vivo. *Neurotherapeutics* **2012**, *9*, 464−476.
(42) Attar, A.; Ripoli, C.; Riccardi, E.; Maiti, P.; Li Puma, D. D.; Liu, T.; Hayes, J.; Jones, M. R.; Lichti-Kaiser, K.; Yang, F.; et al. Protection of Primary Neurons and Mouse Brain From Alzheimer's Pathology by Molecular Tweezers. *Brain* **2012**, *135*, 3735−3748.
(43) Wyttenbach, T.; Kemper, P. R.; Bowers, M. T. Design of a New Electrospray Ion Mobility Mass Spectrometer. *Int. J. Mass Spectrom.* **2001**, *212*, 13−23.
(44) Wyttenbach, T.; Bowers, M. Gas-Phase Conformations: The Ion Mobility/Ion Chromatography Method. In *Modern Mass Spectrometry*; Schalley, C., Ed.; Springer: Berlin, Heidelberg, 2003; Vol. *225*, pp 207−232.
(45) Bernstein, S. L.; Wyttenbach, T.; Baumketner, A.; Shea, J.-E.; Bitan, G.; Teplow, D. B.; Bowers, M. T. Amyloid β-Protein: Monomer Structure and Early Aggregation States of Aβ42 and Its Pro19 Alloform. *J. Am. Chem. Soc.* **2005**, *127*, 2075−2084.
(46) Bleiholder, C.; Dupuis, N. F.; Wyttenbach, T.; Bowers, M. T. Ion Mobility-Mass Spectrometry Reveals a Conformational Conversion from Random Assembly to β-Sheet in Amyloid Fibril Formation. *Nat. Chem.* **2011**, *3*, 172−177.
(47) Gessel, M. M.; Bernstein, S.; Kemper, M.; Teplow, D. B.; Bowers, M. T. Familial Alzheimer's Disease Mutations Differentially Alter Amyloid β-Protein Oligomerization. *ACS Chem. Neurosci.* **2012**, *3*, 909−918.
(48) Roychaudhuri, R.; Lomakin, A.; Bernstein, S.; Zheng, X.; Condron, M. M.; Benedek, G. B.; Bowers, M.; Teplow, D. B. Gly25-Ser26 Amyloid β-Protein Structural Isomorphs Produce Distinct Aβ42 Conformational Dynamics and Assembly Characteristics. *J. Mol. Biol.* **2014**, *426*, 2422−2441.
(49) Baumketner, A.; Bernstein, S. L.; Wyttenbach, T.; Bitan, G.; Teplow, D. B.; Bowers, M. T.; Shea, J.-E. Amyloid β-Protein Monomer Structure: A Computational and Experimental Study. *Protein Sci.* **2006**, *15*, 420−428.
(50) Bleiholder, C.; Do, T. D.; Wu, C.; Economou, N. J.; Bernstein, S. S.; Buratto, S. K.; Shea, J.-E.; Bowers, M. T. Ion Mobility Spectrometry Reveals the Mechanism of Amyloid Formation of Aβ(25−35) and Its Modulation by Inhibitors at the Molecular Level: Epigallocatechin Gallate and Scyllo-inositol. *J. Am. Chem. Soc.* **2013**, *135*, 16926−16937.
(51) Lomakin, A.; Chung, D. S.; Benedek, G. B.; Kirschner, D. A.; Teplow, D. B. On the Nucleation and Growth of Amyloid β-Protein Fibrils: Detection of Nuclei and Quantitation of Rate Constants. *Proc. Natl. Acad. Sci. U. S. A.* **1996**, *93*, 1125−1129.
(52) Gidden, J.; Baker, E. S.; Ferzoco, A.; Bowers, M. T. Structural Motifs of DNA Complexes in the Gas Phase. *Int. J. Mass Spectrom.* **2005**, *240*, 183−193.
(53) Mason, E. A.; McDaniel, E. W. *Transport Properties of Ions in Gases*; Wiley: New York, 1988.
(54) Lee, H. H.; Choi, T. S.; Lee, S. J. C.; Lee, J. W.; Park, J.; Ko, Y. H.; Kim, W. J.; Kim, K.; Kim, H. I. Supramolecular Inhibition of Amyloid Fibrillation by Cucurbit[7]uril. *Angew. Chem., Int. Ed.* **2014**, *53*, 7461−7465.

DOI: 10.1021/acs.jpcb.5b00692
J. Phys. Chem. B 2015, 119, 4831−4841